Inter. Conf. Geol. Arab World (GAW9), Cairo University – March 2008, **p. 76-96.**

GEOCHEMISTRY OF LAMPROPHYRE DYKES IN THE EASTERN DESERT OF EGYPT

Ibrahim, M. E., Ragab, A. A. and Ibrahim, I. H.
Nuclear Materials Authority, Cairo, Egypt.

ABSTRACT

The present work provides original data on two lamprophyre dykes intersecting mineralized shear zones in Abu Hawis and Abu Rusheid, Eastern Desert of Egypt. The Abu Hawis lamprophyre dyke is located at the central Eastern Desert and trending N-S and has 1-10m width and up to 1 km length with vertical dip, cutting peraluminous granites. Abu Hawis lamprophyre dyke is fresh, barren and composed mainly of phynocrysts of amphibole, clinopyroxene and phlogopite with plagioclase and K-feldspars. Chlorite, muscovite and sericite are secondary minerals whereas opaques, apatite, allanite, zircon are accessories. The lamprophyre dyke has relatively alkaline nature and its source magma is rich in LREE and LILE. It is enriched in U, Th, Rb, Zr and Nb relative to primitive mantle. The Nb/Ta ratios (16.6-18.3) and Zr/Hf ratios (39.7-43.5) of the Abu Hawis lamprophyre are similar to primitive mantle (17.5 for Nb/Ta; 35-45 for Zr/Hf).

The REE patterns of the studied lamprophyre dyke in Abu Hawis shows remarkable enrichment is the LREE over the HREE. The absence of Eu anomalies (Eu/Eu* = 0.85-1.09) is due to insignificant role of plagioclase fractionation. However, the non-mineralized (fresh) lamprophyre of Abu Hawis does not show tetrad effect. It could be related to partial melting of upper mantle source with lower crustal contamination during post collision setting and active continental margin in subduction-related setting.

The Abu Rusheid area is located at the south Eastern Desert of Egypt. The Abu Rusheid lamprophyre dyke cuts mylonites, trending E-W, up to 400m long and 2-7 m width with inclined dip (40^{o}/S). The lamprophyre dyke is composed mainly of phynocrysts of pyroxene ,phologopite, hornblende, muscovite, cordierite, sillimanite and kyanite with retrograde metamorphism. Opaques, tourmaline, quartz, fluorite and zircon are accessories. The Abu Rusheid lamprophyre dyke is alkaline and its source magma had ultra-potassic to rarely shoshonite in nature. It's enriched in LILE, Ni, Zn, Pb, Cu, Be, Co, Sn and As.

The ∑REE varies from 25 to 174 ppm with weak to very strong negative Eu anomaly (Eu/Eu*= 0.92–0.01) and LREE/HREE ratio ranging between 0.67 and 1.92. The mineralized lamprophyre dyke of Abu Rusheid shows clear M-type tetrad effect due to the alteration (thermal effect from saturated fluid solution). The presence of negative Ce anomaly in Abu Rusheid lamprophyre samples suggests mobilization of REE under supergene conditions. The studied lamprophyre dyke had alkaline magma nature and formed in subduction-related setting and active continental margin.

Key words; lamprophyre, Abu Rusheid, Abu Hawis, REEs, tetrad effect, uranium.

1- INTRODUCTION

Lamprophyres, a unique type of melanocratic hypabyssal igneous rock, characterized by microporphyritic textures with mafic phenocrysts (Rock, 1991), are widespread in various tectonic settings (Madhavan et al., 1998), and are considered to have close temporal-spatial relationships to gold mineralization in some large- and super large-sized gold districts (Huang et al., 2002). Their petrogenesis is complex and diverse, and they are generally classified into three models: (1) partial melting of metasomatic and enrichment of the mantle (Zhang et al., 2003), either in a subduction related environment (Huang et al., 2002) or in the sub-continental lithospheric mantle (Fowler and Henney, 1996); (2) continental crust contamination of mafic magmas (Currie and Williams, 1993); or

(3) mixing of upwelling basaltic magma with varying amounts of ultrapotassic lithospheric-mantle melts that is related to heating and/or thinning of sub-continental lithospheric-mantle (Thompson et al., 1990), or of mantle-derived basaltic or lamproite melts and crustally derived silica melts (Prelevic et al., 2004).

Altered lamprophyre dykes are generally considered as good traps (physical and chemical) for polymineralization. The alteration of feldspars to clay minerals are considered as chemical traps, while the alteration of pyrites, olivine and quartz leaves rounded to semi-rounded vugs (boxworks) are considered as physical traps.

Lamprophyres are group of dark colored, porphyritic, hypabyssal igneous rocks and characterized by a panidiomorphic texture forming both the phenocrysts and the fine-grained groundmass. They typically occur in thin dykes or sills and have low SiO_2 (mostly 40 to 47%), high (MgO + FeO) and (Na_2O + K_2O) (Carmichael et al., 1974). Lamprophyres are divided into five main categories (Streckeisen, 1979; Le Maitre, 1989; Rock, 1991). These are (i) calc-alkaline lamprophyres (CAL); ii) alkaline lamprophyres (AL), iii) ultramafic lamprophyres (UML), iv) lamproitic lamprophyres (LL) and v) kimberlitic lamprophyres. The calc-alkaline types usually are found in convergent tectonic environments, whereas alkaline and ultramafic types are associated with anorogenic extensional and divergent tectonic environments settings. Kimberlites are characteristic of within-plate settings (Carlier et al., 1997). Recently Ibrahim et al. (2006 and 2007a, b & c) recorded N-S lamprophyre dykes bearing REE, Zn, Cu and U-minerals in Abu Rusheid area.

The present study is concerned with geochemical characteristics of two different lamprophyre dykes in two different shear zones; Abu Hawis at the central Eastern Desert and Abu Rusheid at the south Eastern Desert of Egypt .

2- GEOLOGICAL SETTING

1- Gabal (G.) Abu Hawis covers about 126 km^2, elliptical in shape following NNW-SSE trend (Fig.1). Abu Hawis area is located in the Central Eastern Desert of Egypt .The area is outlined by latitudes 26˚ 42' 45" - 26˚ 45' 45" N and longitudes 33˚ 34' 37" - 33˚ 38' 06" E. The Abu Hawis lamprophyre dyke is trending N-S and has 1-10m width and up to 1 km length with almost vertical dip, cutting peraluminous granite. All granitic rocks of the area (older and younger granitic rocks) are dissected by post-granite dikes (basic, intermediate and acidic) and veins, and traversed by numerous variable faults in trend and length. The older granitoids constitute about 85% of the total area and represented by granodiorite and tonalite-trondhjmite in composition (Moustafa, 2007).

The younger granites (fine to medium–grained) cover about 8 km^2 with sharp contact with the former, range in color from pink to reddish pink and composed of quartz, perthites, plagioclase, muscovite and biotite .Epidote and chlorite are secondary minerals, whereas apatite, zircon, monazite and opaques are accessories. Two granitic phases (syenogranite and monzogranite) are differentiated in the field; the peripheral phase is formed of medium- grained biotite-granites (syenogranite), whereas the core phase of the mass is formed of medium-grained muscovite-biotite granite (monzogranite). The younger granites show high eU-contents with an average equal to 23 ppm and e(U/Th) ratio varies from 1.6 to 2.9 (Moustafa, 2007).

Gabal Abu Hawis is affected by NE-SW, NW-SE, N-S and E-W fault systems which partly filled with basic dikes, aplite dikes, pegmatite pockets and quartz veins. The northern part of the Abu Hawis pluton is affected by NE-SW discontinuous mineralized shear zone with secondary uranium intersected by left-hand NW-SE strike-slip faults (Darwish, 2008). The N-S lamprophyre dike cuts both the younger granites and its NE-SW shear zone (Fig. 1). Abu Hawis lamprophyre dike (up to 10 m in width) is, black in color, owing to the abundance of ferromagnesian ,fresh, barren and mainly composed of phenocrysts of amphibole, phlogopite and pyroxene, set in fine-grained groundmass. Feldspars, chlorite,

muscovite and sericite are secondary minerals. Opaques, apatite, allanite, corundum and zircon are accessories.

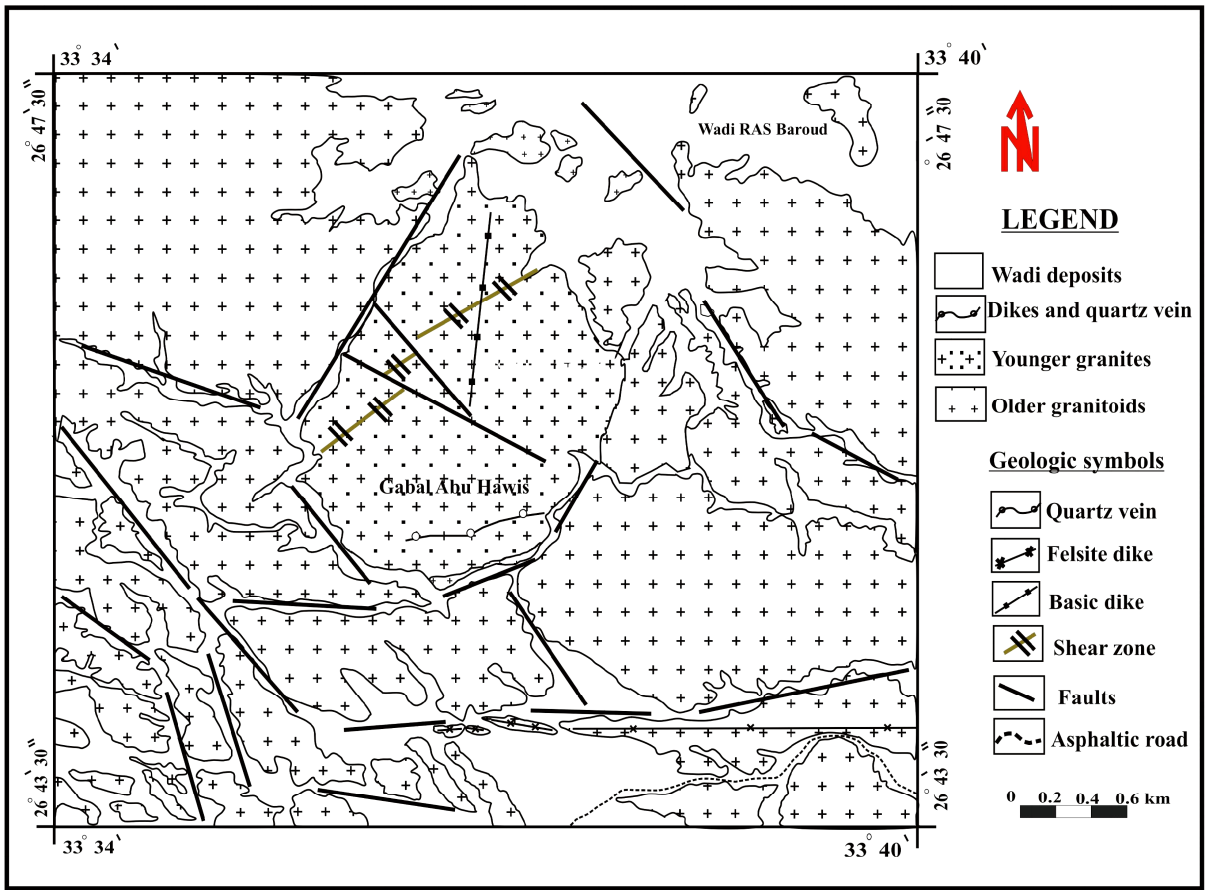

Fig.(1) : Geologic map of Gabal Abu Hawis area, after Moustafa, (2007).

2- Abu Rusheid area is located 50 km southwest of Marsa Alam from the Red Sea coast. Abu Rusheid rocks are classified into cataclastics with common banding and high foliation (mainly composed of protomylonite, mylonite, ultramylonite and silicified ultramylonite with gradational contacts). They are cut by two sets (N-S and E-W trends) of lamprophyre dykes-bearing mineralization e.g. U, REE, Cu, Zn & Pb (Ibrahim et al., 2006, 2007a, b & c). Abu Rusheid area is traversed by good channel-ways represented by strike slip faults trending ENE-WSW, NNW-SSE, N-S and NNE-SSW ,

A lamprophyre dyke (E-W trend, 400 m in length and ranges from 2-7 m in width with dip 4^{O} due to S-direction) cuts cataclastic rocks (Fig. 2) with common boxworks and tourmaline crystals up to 2 cm in length. Petrographically, lamprophyre is a coarse-grained, hard, massive and grayish-green in color. It is mainly composed of hornblende, phologopite, plagioclase, cordierite, sillimanite, kyanite and relics of muscovite. Opaques, tourmaline, fluorite, quartz, prehnite and zircon are accessories. The alteration products are represented by chlorite.

3- GEOCHEMISTRY

Thirteen samples were analyzed using a Philips PW-2400 X-ray fluorescence spectrometer (XRF). The uncertainties of analyses are 1-2 % for the major elements and around 1-3 % for the trace and REE elements. All chemical analyses were carried out in

the Laboratories of the ACME analytical, Vancouver, Canada. The geochemical data are presented in tables (1 & 2).

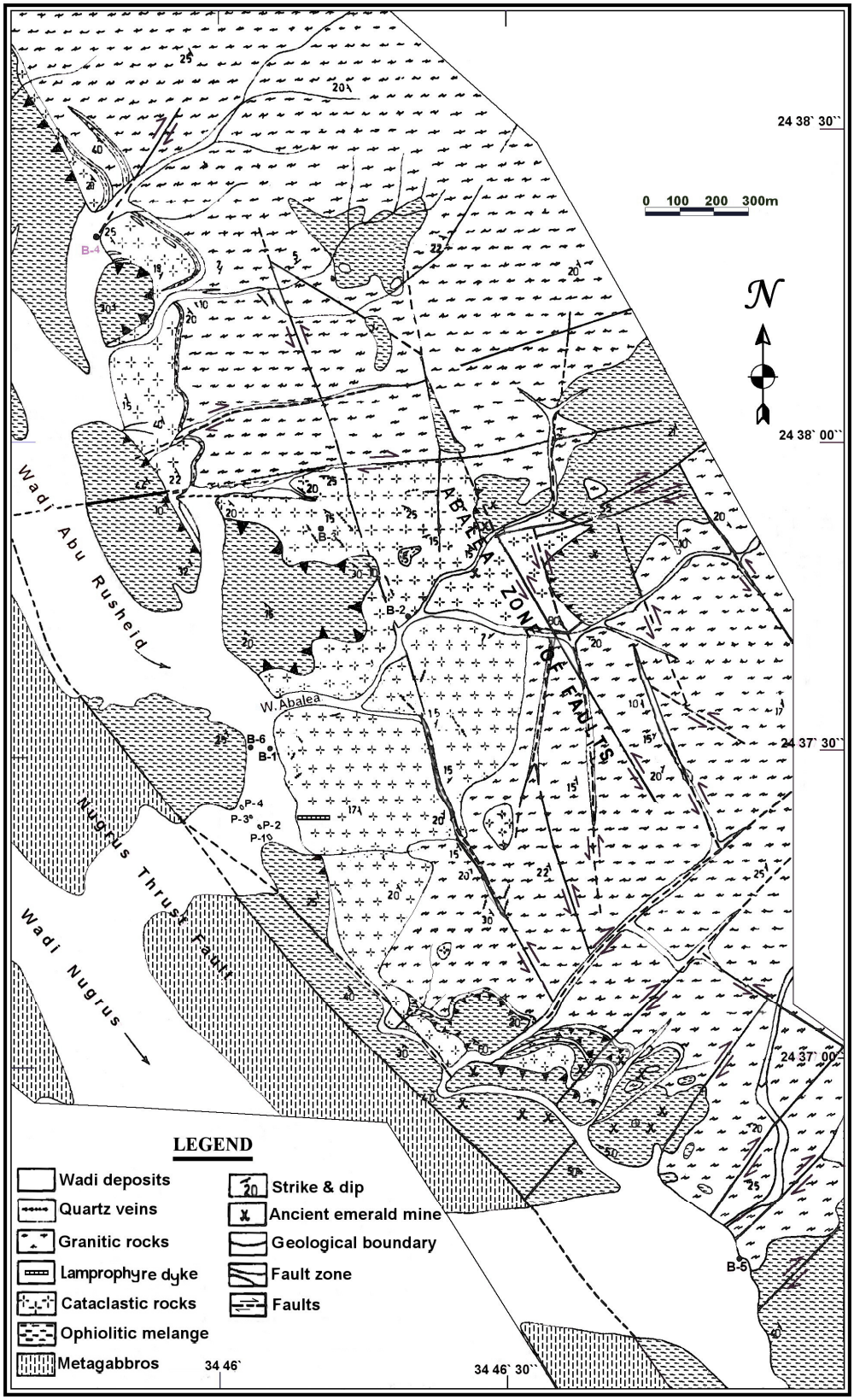

Fig. (2): Geologic map of Abu Rusheid area, South Eastern Desert, Egypt, after Ibrahim et al., (2006).

Geochemical Characteristic:

Abu Hawis lamprophyre dyke is characterized by its low SiO_2 (44.41-52.23 %), and high Al_2O_3 (12.3-14.49 %), CaO (4.99-12.09 %), Fe_2O_3 (13.78-18.16 %), TiO_2 (2.42-3.43 %), P_2O_5 (1.7-2.32 %), LREE (253.4-317.59 ppm), HFSE (Zr, Y and Nb) and LILE (Sr and Ba) (Table1).

The Abu Rusheid lamprophyre dyke samples have abnormal contents of Pb (35-190 ppm), Zn (335->10000), Ni (206-517 ppm), Co (32-69 ppm), V (67-77 ppm), Sn (55-205 ppm), Cs (27-50 ppm) and As (7-122 ppm) (Table. 2).

The Rb/Sr ratio is an important criterion to distinguish between magmas coming either from the upper crust (Rb/Sr= 0.25), lower crust (Rb/Sr= 0.03 -0.09) or from the upper mantle (Rb/Sr= 0.02 – 0.04) (Schroll, 1976). Abu Hawis lamprophyre dyke shows lower Rb/Sr ratio (0.01- to 0.91) which may reflect upper mantle – lower crust origin of their parent magma. (Table. 1).

However, the lamprophyre dyke in Abu Rusheid shows (Rb/Sr) ratio varies from (14.39 to 53.17) due to the alkaline metasomatism process. In addition, subducted sediment can be significantly enriched in Rb over both Sr and Ba in the mantle (Chung et al., 2001). Consequently, the degree of Rb enrichment is higher than those of Sr and Ba, indicating that source contaminated by sediment via subduction would be responsible for the Abu Rusheid lamprophyre dyke.

The Nb/Ta ratio (16.6-18.3) and Zr/Hf ratio (39.7-43.5) in the Abu Hawis lamprophyre dyke are similar to primitive mantle (17.5 for Nb/Ta, Zr/Hf 35-45) (McDonough and Sun, 1988) and lie in the mantel sub-continental lithosphere field. However, Abu Rusheid lamprophyre dyke have non-chondrtic Zr/Hf (21.1-35.1), Y/Ho (23.9-6.8) and Nb/Ta (9.2-30) ratios due to hydrothermal alterations.

Incompatible isovalent ratios are usually utilized to characterize crustal contamination. The average Nb/U ratios for upper and lower crust are 9 and 21, respectively. MORB and OIB show nearly constant Nb/U ratios (10 to 47, Hofmann et al., 1986), whereas the Nb/U ratio for the rocks contaminated by crust is from 9 to 40 (Ge et al., 2001). The studied Abu Hawis lamprophyre dyke is contaminated by curst (Nb/U 9-40).

The REE of the studied Abu Hawis lamprophyre dyke are characterized by low Ce anomalies (0.88-0.91), LREE enrichment [ΣLREE= (253.4-321.4) & $(La/Sm)_n$= (2.1-2.36), $(Ce/Yb)_n$= (3.42-5.98)] and depleted in HREE [(ΣHREE= 38.11-51.45) & $(Tb/Yb)_n$= (1.26-2.07)]. However the Abu Rusheid lamprophyre dyke has negative Ce anomalies (0.47-0.9) due to the mobilization of REEs under supergene conditions also the samples are enriched in the HREE [(ΣHREE= 8.59-92.68) & $(Tb/Yb)_n$= (0.38-0.47)] and depleted in LREE [ΣLREE= 16.49-91.16 $(La/Sm)_n$= 0.84-1.48) & $(Ce/Yb)_n$= 0.21-0.47].

Magma Type

The chemical classification and nomenclature depicting lithological variation of the studied lamprophyres on total alkalis versus silica diagram after Cox et, al., (1979). The samples show more evolved lithologics including Hawaiite, Tephrite basalts (Abu Rusheid lamprophyre) ,basalt and basalt andesite (Abu Hawis lamprophyre) (Fig. 3).

Their K_2O/Al_2O_3 ratio is much lower than those of lamproite (usually $K_2O/A1_2O_3$ **>** l) (Shu, 1994). On a SiO_2 versus (K_2O + Na_2O) diagram (Fig. 4) all samples plot in the field of alkaline lamprophyre and lamproite field (Fig, 4) (Lu et al., 1991).

Table (1): Results of major oxides (wt %), some trace elements (ppm) and REE (ppm) of lamprophyre dyke, Abu Hawis area, Central Eastern Desert, Egypt.

Sample	AB1	AB2	AB3	AB4	AB5	AB6	AB7
Oxides elements (wt.%)							
SiO_2	46.82	48.07	52.32	45.84	46.39	44.41	44.84
Al_2O_3	13.64	13.96	12.3	14.1	13.22	14.49	13.92
Fe_2O_3	14.76	13.78	14.57	16.4	17.23	16.38	18.16
MgO	3.62	3.56	2.95	4.3	4.55	3.79	3.47
CaO	12.09	11.68	5.14	5.17	4.98	5.35	4.99
Na_2O	0.07	0.16	2.18	2.8	2.38	2.69	1.89
K_2O	0.15	0.27	0.8	1.23	0.78	1.05	1.24
TiO_2	2.89	2.73	2.42	3.27	3.43	3.26	3.25
P_2O_5	2.02	1.88	1.7	2.32	2.41	2.32	2.28
MnO	0.23	0.21	0.3	0.27	0.28	0.26	0.35
Cr_2O_3	0.004	0.002	<.001	<.001	0.002	<.001	<.001
L.O.I.	3.4	3.4	5.1	4	4.2	5.8	5.4
Total	99.7	99.7	99.79	99.71	99.85	99.8	99.79
Trace elements (ppm)							
Sc	20	18	21	23	25	22	22
Mo	3.4	3	2.5	2.2	3.9	5.2	3.5
Cu	10.5	4.8	2.9	14.5	19.3	1.4	1.1
Pb	2.1	6.1	2.3	1.5	1.4	1.3	2.9
Zn	199	212	169	212	223	98	110
As	<.5	1.3	<.5	<.5	<.5	<.5	<.5
Cd	0.1	<.1	0.1	0.1	<.1	0.1	0.1
Ag	<.1	<.1	<.1	<.1	<.1	<.1	<.1
Au	1.5	1.3	2	5.6	1.7	2.3	1.3
Ba	27.8	45.9	125.4	737.1	447.3	112.6	113.3
Be	2	4	3	3	3	4	3
Co	30.7	27.1	23.3	37.8	37.4	29.5	25.3
Cs	0.3	0.4	0.6	0.2	0.3	0.5	0.6
Ga	26.5	36.4	34.1	29.3	29.7	27.6	26.3
Hf	8	6.8	10.7	9.8	9.6	8.2	9
Nb	54.9	48.9	63.7	66.2	65.7	59	60.6
Rb	9.5	16.8	55.6	62.4	40.9	74.2	109.2
Sn	2	2	2	2	2	2	2
Sr	1112.6	1119.4	88.5	143.2	157.2	114.2	119.8
Ta	3	2.8	3.6	3.9	4	3.5	3.4
Th	5.7	3.7	6.9	5.2	6.5	6.6	5.9
U	2.7	2.5	4.8	3.4	3.4	5.4	3.8
V	145	164	94	143	149	145	161
W	1.6	2.2	2.1	1.2	1.3	1.6	2.7
Zr	328.5	297.1	442.9	392.9	405.6	357.2	357.4
Y	64.8	57.8	81.3	80.5	78.9	71.1	91.8
La	55.6	49.3	53.8	60.7	62.3	58.6	54.2
Ce	111.9	103.1	112.7	126.1	127.7	118.9	116.1
Pr	16.6	14.98	16.53	19.04	19.34	17.73	17.37
Nd	76.4	68.2	75.5	88.3	88.8	82.5	81.5
Sm	15.09	13.28	15.14	17.67	17.53	15.61	16.22
Eu	5.07	4.54	4.07	5.78	5.76	4.98	5.05
Gd	13.56	11.85	13.7	15.84	15.79	13.72	15.43
Tb	2.24	2	2.44	2.68	2.66	2.28	2.59
Dy	11.36	10.24	13.41	13.66	13.41	11.47	12.69
Ho	2.13	1.91	2.66	2.59	2.48	2.24	2.5
Er	5.73	5.31	7.88	6.87	6.88	6.43	6.55
Tm	0.84	0.81	1.32	1.02	1.02	1.03	0.96
Yb	4.85	5.13	8.52	6.11	6.2	6.04	5.5
Lu	0.8	0.86	1.52	0.98	1.01	1.04	0.9

Table (1) Content:

Sample	AB1	AB2	AB3	AB4	AB5	AB6	AB7
ΣREE	322.4	291.51	329.19	367	370.88	342.57	337.56
Eu^*	1.06	1.09	0.85	1.04	1.04	1.02	0.96
Ce^*	0.88	0.91	0.9	0.89	0.88	0.88	0.91
ΣLREE	280.66	253.4	277.74	317.59	321.43	298.32	290.44
ΣHREE	41.51	38.11	51.45	49.75	49.45	44.25	47.12
LREE/HREE	6.76	6.64	5.39	6.38	6.5	6.74	6.16
T1	0.93	0.96	0.96	0.94	0.94	0.93	0.95
T3	1.02	1.03	1.03	1.03	1.04	1.0	1.0
$TE_{1,3}$	0.975	0.995	0.995	0.985	0.99	0.965	0.975
Zr/Hf	41.06	43.69	41.39	40.09	42.2	43.5	39.7
Y/Ho	30.0	30.4	30.5	31	31.8	31.7	36.7
Nb/ Ta	18.3	17.46	17.69	16.94	16.42	16.8	17.8
Rb/ Sr	0.0085	0.15	0.628	0.705	0.260	0.124	0.911
Th / U	2.1	1.4	1.43	1.5	1.8	1.2	1.5
Nb / U	20.3	19.56	13.2	17.7	19.3	10.9	15.9
$(La / Sm)_n$	2.317	2.33	2.23	2.16	2.23	2.36	2.10
$(Ce / Yb)_n$	5.98	5.49	3.42	4.77	5.26	5.09	5.44
$(Tb / Yb)_n$	2.03	1.8	1.26	1.93	1.89	1.66	2.07

Table (2): Results of major oxides (wt %), some trace elements (ppm) and REE_S (ppm) of lamprophyre dyke, Abu Rusheid area, South Eastern Desert, Egypt.

Sample	8PT	7PT	6PT	3PT	2PT	1PT
Oxides elements (wt%)						
SiO_2	46.33	47.24	46.07	46.37	45.75	46.03
Al_2O_3	11.3	9.91	12.98	12.24	12.65	12.54
Fe_2O_3	8.75	9.28	9.21	9.2	9.27	9.46
MgO	19.76	18.12	16.3	16.57	17.62	17.42
CaO	5.08	9.06	2.66	3.3	2.16	2.14
Na_2O	1.05	1.12	1.17	0.59	0.42	0.41
K_2O	5.08	3.41	7.15	7.9	8.78	8.63
TiO_2	0.34	0.15	0.28	0.26	0.24	0.23
P_2O_5	0.04	0.05	0.08	0.02	<.01	0.04
MnO	0.21	0.15	0.13	0.2	0.21	0.2
Cr_2O_3	0.194	0.179	0.144	0.148	0.148	0.148
L.O.I.	1.6	1.1	1.8	2.5	2.1	2.1
TOT/C	0.08	0.19	0.22	0.03	0.02	0.02
TOT/S	0.02	0.1	0.02	0.04	0.05	0.04
SUM	99.84	99.83	98.04	99.35	99.4	99.41
Trace elements (ppm)						
Ba	569.2	123.8	164.2	901.5	201.4	193.1
Be	33	20	20	18	21	20
Co	54.1	68.6	40	35.7	31.9	34.6
Cs	29.8	26.8	51.9	46	50.1	50.1
Ga	18.2	15.7	15.1	16.7	16.7	16.7
Hf	5.3	<.5	2.7	3.5	1.7	1.7
Nb	28.7	18	33.1	35.7	35.2	36.3
Rb	621.7	526.7	1245.4	1629.2	1824	1851.6
Sn	122	205	55	104	107	109
Sr	30	36.6	82.1	49.9	34.3	35.9
Ta	3.1	0.6	1.5	3.5	3.5	3.7
Th	8.4	2.5	16.6	22.7	13.8	13.7
U	1.9	0.5	2.8	6.9	7.2	7.2
V	117	67	77	72	72	76
W	0.8	35.8	1.4	6	3.5	3.6
Zr	111.5	10.6	94.6	92.8	56.5	56.9
Y	76	15.1	60.7	104.7	115.1	116.5
Mo	0.6	0.4	10	23	21	22
Cu	14.6	6	115	191	207	204
Pb	32.1	35	120	186	190	188
Zn	599	335	>10000	2640	2975	2990
Ni	517	206	369	353	329	331
As	15	7	133	111	122	122
Cd	0.2	0.5	5	1.5	1	1
Sb	<0.1	0.1	0.1	0.3	0.2	0.2
Bi	0.3	0.7	0.2	1.3	1	1
Ag	<0.1	<0.1	0.1	1.4	0.9	1
Hg	<0.1	<0.1	0.01	0.01	<0.1	0.02
Tl	3.2	2.5	6	8	8	8
Se	0.5	0.5	<0.5	1.1	1.3	1.1
Sc	23	16	17	18	18	18
REEs (ppm)						
La	4.5	4.2	11.4	18.4	16.1	16
Ce	9.8	4.5	18	35.9	25	25.3
Pr	1.88	1.08	4.1	6.83	6.33	6.23
Nd	9	5.3	15.1	22.9	20.4	19.7
Sm	2.97	1.05	3.66	6.78	6.84	6.96
Eu	0.85	0.36	0.36	0.35	0.27	0.32
Gd	4.57	1.17	3.84	6.28	6.79	6.78
Tb	1.28	0.26	1.18	2.37	2.68	2.68
Dy	9.91	1.79	8.05	17.19	19.51	19.9
Ho	2.54	0.41	1.99	4.36	4.82	4.79
Er	9.37	1.58	8.19	17.67	19.51	19.79
Tm	1.79	0.3	1.83	3.69	4.19	4.13
Yb	11.86	2.43	12.26	26.99	30.14	30.11
Lu	1.92	0.45	2.06	4.02	4.59	4.5

Table (2) Content:

Sample	8 PT	7 PT	6 PT	3 PT	2 PT	1 PT
ΣREE	72.24	25.08	92.47	173.73	167.17	167.19
Eu^*	0.7	0.92	0.29	0.16	0.12	0.14
Ce^*	0.83	0.47	0.69	0.87	0.68	0.71
ΣLREE	29	16.49	52.62	91.16	74.94	74.51
ΣHREE	43.24	8.59	39.85	82.57	92.23	92.68
LREE/HREE	0.67	1.92	1.32	1.10	0.81	0.8
T1	0.95	0.55	0.92	1.08	0.98	1.09
T3	1.14	0.99	1.25	1.33	1.37	1.39
$TE_{1,3}$	1.04	0.80	1.07	1.2	1.2	1.2
Zr/Hf	21.0	26.5	35.0	26.5	32.7	33.5
Y/Ho	29.9	36.8	30.5	24	23.9	24.36
Nb/ Ta	9.25	30	22	0.05	9.8	9.8
Rb/ Sr	20.7	14.39	15.16	32.64	53.17	44.05
Th / U	4.4	5.7	5.0	1.0	1.9	1.9
Nb / U	15.1	36	11.8	5.1	4.8	5.04
$(La / Sm)_n$	0.95	0.88	1.96	0.84	1.48	1.44
$(Ce / Yb)_n$	0.12	0.47	0.22	0.34	0.21	0.21
$(Tb / Yb)_n$	0.47	0.47	0.24	0.38	0.39	0.39

Lamprophyre samples of Abu Rusheid lie within the overlapping fields of lamproite and lamprophyre (Fig. 5) while Abu Hawis samples lie in and out lamprophyre field. In CaO-Al_2O_3 diagram of Foley et al., (1987). The analyzed samples plot mainly in fields III & I (lamprophyre and lamproite, Fig.6) for Abu Hawis and Abu Rusheid, respectively. The MgO - SiO_2 diagram (after Downes et al., 2005) shows that the Abu Rusheid lamprophyre samples is highly magnesium (>16 wt% MgO) compared with Abu Hawis (5 wt% MgO). On diagram (Fig. 7), the cumulate rocks appear as mixtures of their constituent minerals (i.e. between diopside, olivine, nepheline, calcite, dolomite, phologopite and melilite). The Abu Rusheid lamprophyre samples plot between diopside and phologopite minerals indicate more mafics silicate phases, whereas Abu Hawis samples lie between nepheline and melilite minerals.

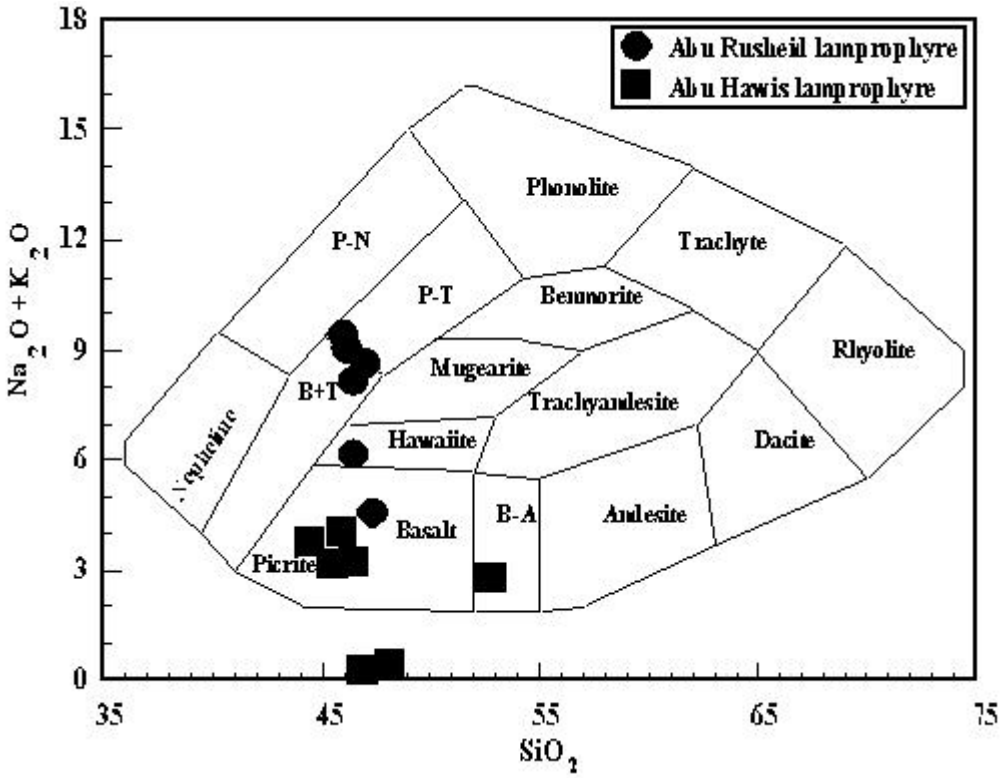

Fig. 3: Weight % alkali oxides vs. wt % SiO_2 of Cox et al. (1979). B+T= Basalts and Tephrites, P-T= Fonalitic Tephrites, P-N= Fonalitic Nephelenites.

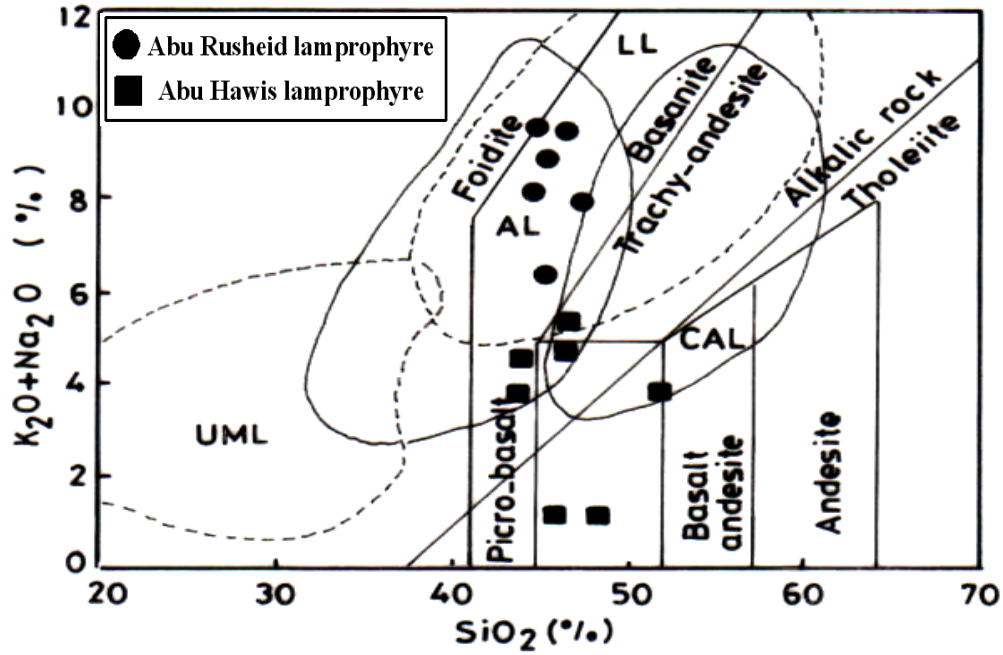

Fig. 4: Plot of SiO_2 versus (K_2O + Na_2O), (after Lu et al., 1991) UML= ultramafic lamprophyre, AL= alkali lamprophyre, CAL= calc-alkaline lamprophyre and LL =lamproite.

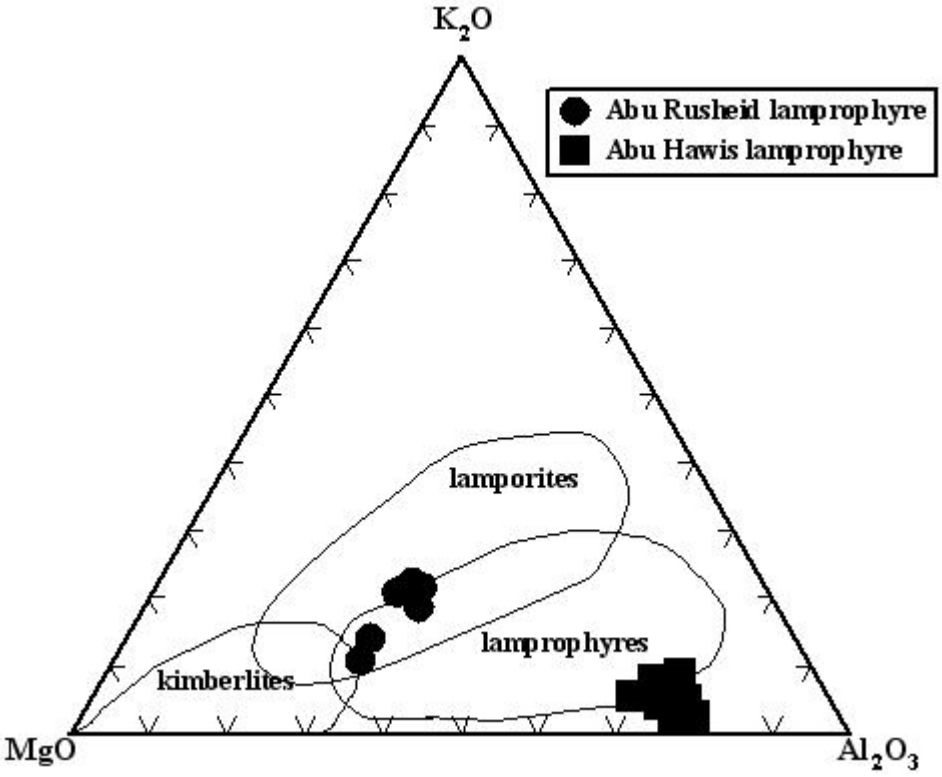

Fig. 5: Ternary plot of K_2O–MgO–Al_2O_3 after Moayyed et al., (2006).

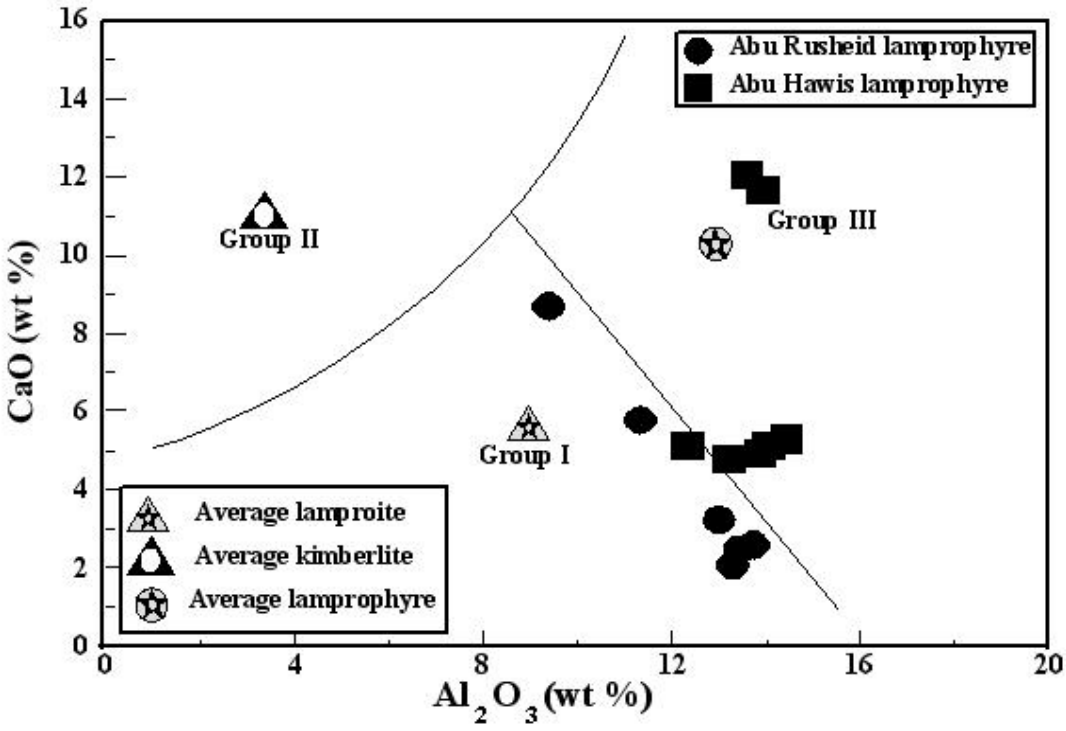

F. 6: CaO (wt%) vs. Al_2O_3 (wt%) diagram after Foley et al., (1987).

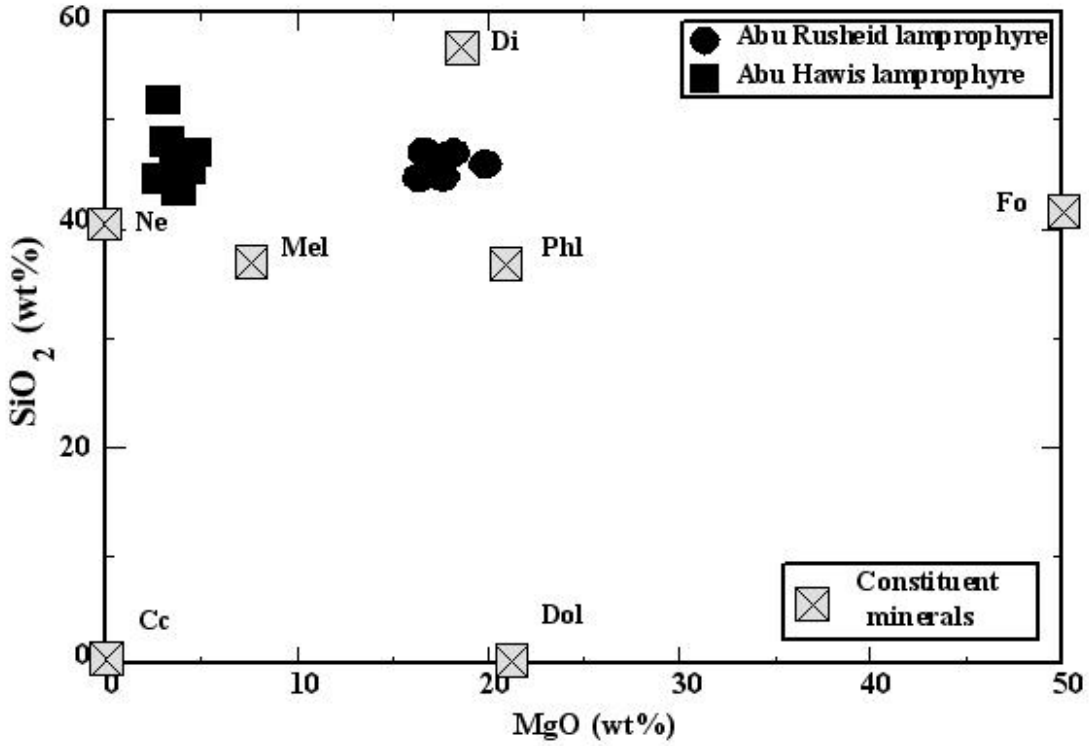

Fig. 7: Variation diagrams of wt% MgO vs. wt% SiO_2 (after Downes et al., 2005) for lamprophyre dykes. Mineral abbreviations: Cc= calcite, Dol= dolomite, Mel= melilite, Fo= forsterite, Di= diopside, Ne= nepheline and Phl= phologopite.

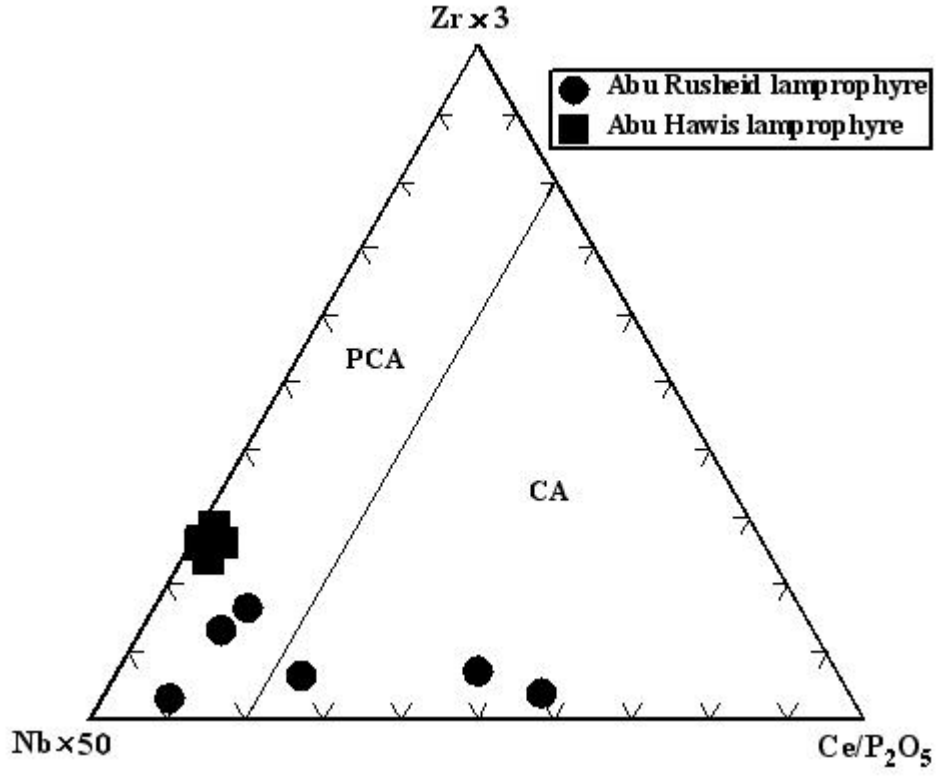

Fig. 8: Nb*50-Zr*3-Ce/P_2O_5 Ternary diagram discriminating the tectonic setting of the studied lamprophyres, after Moayyed et al., (2006).

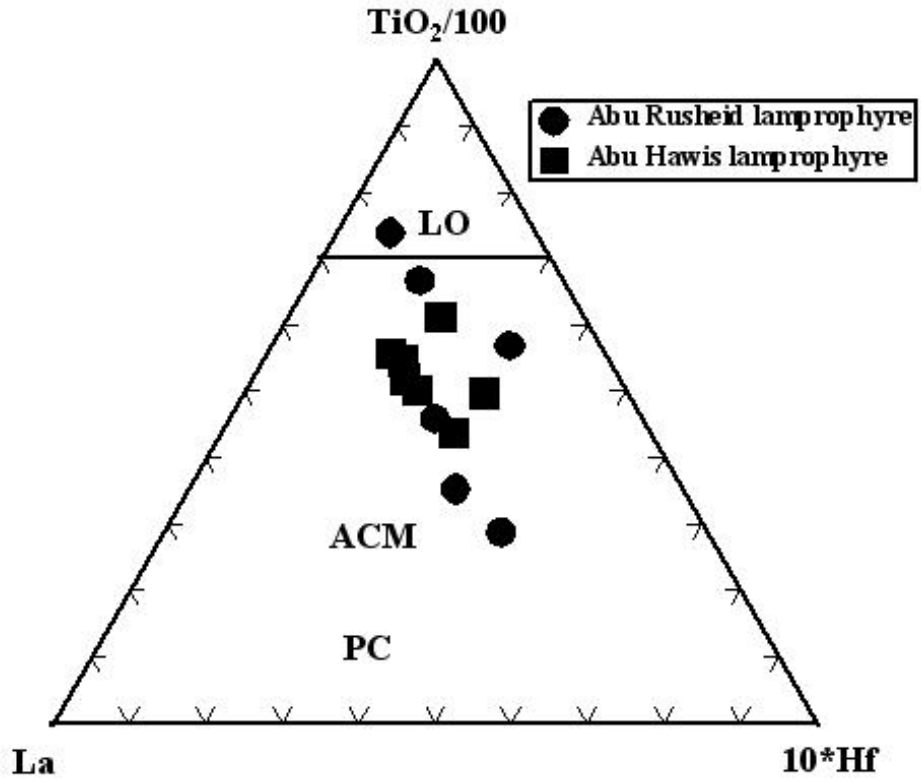

Fig. 9: Tectonic setting discrimination diagram (Muller and Groves, 1997). ACM=Active continental margin and PC= Post-collision setting.

Tectonic setting

The Nb*50-Zr*/3-Ce/P_2O_5 ternary diagram discriminate the tectonic setting of the studied lamprophyres after Moayyed et al., (2006) shows that the studied dyke plot in the post-collision volcanic arc (Fig. 8) .The discrimination diagrams of Muller and Groves (1997) are employed to distinguish the tectonic environment of the studied lamprophyre dykes. The studied samples plot in the post-collision and active continental margin fields (Fig. 9).

Normalized Trace and Rare Earth Elements

The average concentration of trace element relative to the continental crust is enriched in LIL and has distinct negative Nb anomalies (Terney and Weaver, 1987).The two lamprophyre dykes has been normalized to primitive mantle after McDonough and Sun (1988). Figure (10) shows that, the Abu Rusheid lamprophyre samples are enriched in LIL elements with slightly decrease from Rb to Y with strong troughs of Ta, Hf and Ti compared with Abu Hawis samples.

The studied dyke shows strong enrichment in the high incompatible elements (Rb, Th, U, K, La, Ce) relative to the moderate incompatible element, especially (Sm, Nd, Tb, Y, Zr) with significant negative Ba, Hf, Ta and Ti anomalies (characteristic of a anorogenic magmatism (Whalen et al., 1996). In addition, it shows strong similarities to oceanic island basalt (OIB) fractionated lavas. A slightly positive anomaly of Nb and Zr may be a characteristic of enriched mantle behavior (Gaonach et al., 1992) .Thompson (1986) and Fitton (1987) suggested a subcontinental lithospheric mantle source for continental alkali-provinces.

The Ti negative anomalies in Abu Rusheid lamprophyre dyke indicate the removal of titano-magnetite minerals by fractionation from the melt. The normalized patterns of the lamprophyre dykes could reflect enriched mantle source.

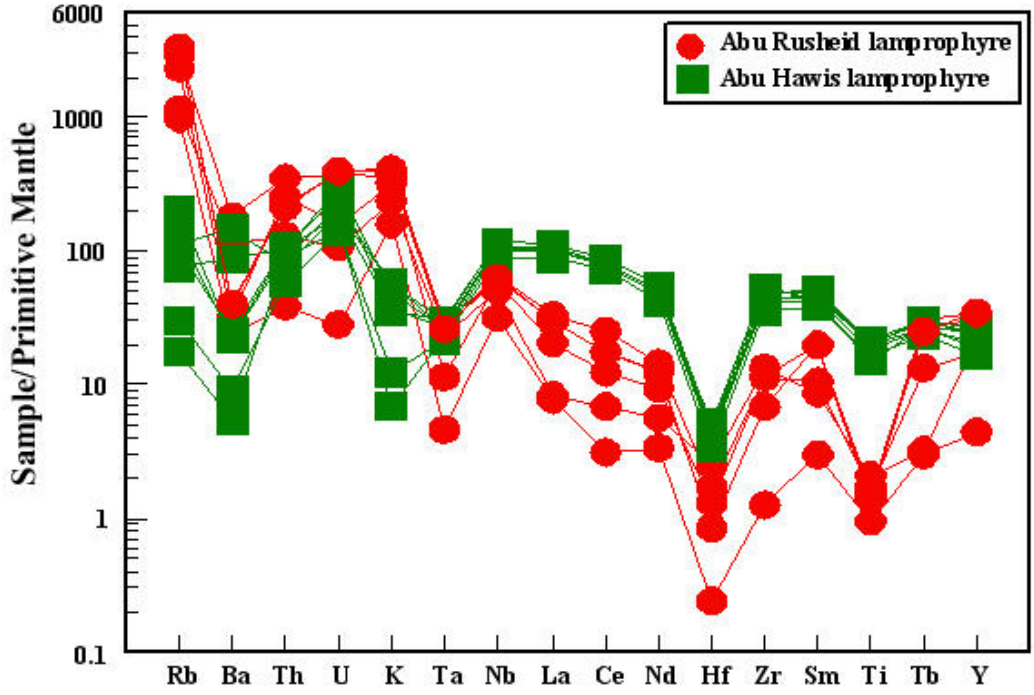

Fig. (10): Incompatible element abundances, normalized to primordial mantle values (McDonough and Sun, 1988) for lamprophyre dykes.

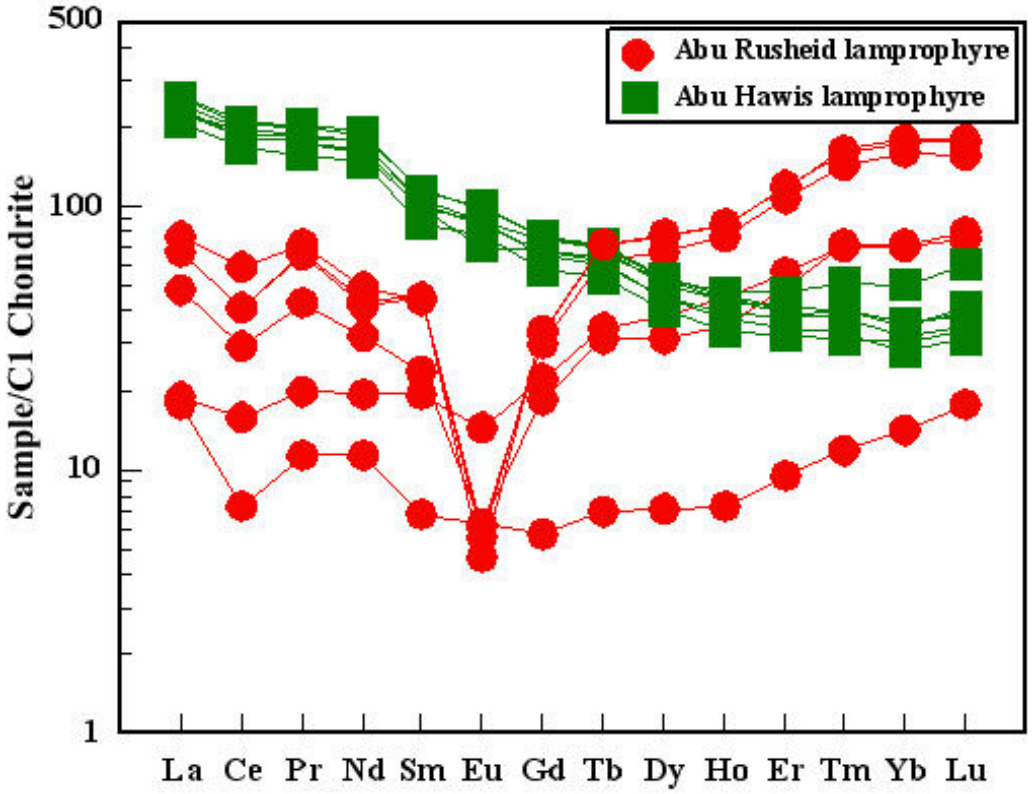

Fig. 11: Chondrite-normalized REE patterns of the studied lamprophyre. Chondrite after Sun and McDonough (1989).

Rare Earth Elements

The Abu Hawis lamprophyre dyke shows ∑REE varies from 292-370 ppm with weak Eu anomalies (Eu/Eu* = 0.85-1.09) and the LREE/HREE ratio ranges from 5.4 to 6.8 whereas LREE enrichment is related to the presence of monazite (McLennan et al., 1979). However, the non-mineralized (fresh) lamprophyre dyke does not show tetrad effect (Fig, 11).

The Abu Rusheid lamprophyre samples (Fig. 11) are characterized by negative Eu anomalies variable varies ΣREE (25-174 ppm) and LREE/HREE ranging from 0.67 to 1.92. Eu anomaly could be related to REE mobility (Taylor and Mclennan, 1980), to Eu leaching by the volatile phase (Taylor et al., 1981) or attributed to sericitization (Alderton et al., 1980). The HREE enrichment is attributed to some heavy minerals (e.g., xenotime, zircon and fluorite).

The REE pattern of lamprophyre dyke displays M-type tetrad effect (Figs. 11 & 12) reflecting possible alteration processes. All lamprophyre samples show $-\Delta Eu < 1$ and $-\Delta Ce < 1$ anomalies indicating scarcity of plagioclases and that the alteration fluids were reducing (Mahdy and El Kammar, 2003).

Tetrad effect

The tetrad effect typically occurs in highly evolved silicate magmas and is attributed to strong fluid-rock interaction. It becomes visible in chondrite-normalized REE patterns. Masuda et al., (1987) classified the four tetrads as: T1 = La-Nd, T2= (Pm) Sm- Gd, T3 = Gd-Ho and T4= Er- Lu which can be either M- or W-shaped.

The REE mobility is controlled by pH, high water/rock ratios and abundant complexing ions CO_3^{2-}, F^-, Cl^-, PO_4^{2-}, SO_4^{2-}, (Hass et al., 1995). The tetrad effect does not play any role in the fresh lamprophyre dyke in the Abu Rusheid and Abu Hawis since its values ($T_{1,3}$) are usually well below (1.2) (Irber, 1999). However, the altered lamprophyre dyke in the Abu Rusheid constantly display pronounced tetrad effects with values as high as 1.2 (Fig 12). In all analyzed samples, the tetrad effect describes a convex (M-shaped) pattern. However, Veksler et al., (2005) concluded from tetrad patterns involving the distribution coefficient that only silicate melts produce M-shaped patterns. The conjugate fluoride liquid, however, should have a W-shape, which is not in accordance with the studied samples.

Chondrite–normalized REE patterns in the studied altered Abu Rusheid lamprophyre dyke (samples No. 6PT, 3PT, 2PT & 1PT) display tetrad effect of M type and marked negative Eu anomaly (Eu/Eu*= 0.12-0.29) due to alteration (thermal effect from saturated fluid solution) and alkali process metasomatism.

However the fresh lamprophyre samples in the Abu Rusheid (samples No 8PTA & 7PT) (Fig. 14) doesn't show the tetrad effect with mild Eu anomalies (Eu/Eu*= 0.7-0.92)

The chondrite-normalized pattern of the altered sample is divided by fresh sample pattern (Fig.13). The obtained diagram reflects the addition of the REE due to alteration by saturated fluid (pegmatitic).

The relationship between Eu anomaly and the REE of both the fresh and altered lamprophyre samples in the Abu Rusheid (Fig.14) shows that, the Eu anomaly shows strong negative correlation with the total REE. However the Eu anomaly shows strong positive correlation with the LREE (Fig 15).

The pronounced tetrad effect in altered lamprophyre dyke of Abu Rusheid suggests that the alteration occurred by highly saturated fluid evolved from pegmatite melts which strongly interacted with F-rich fluid (Zhao et al., 2002, Liu et al., 2005; Irber, 1999. The tetrad effect cannot be explained by fractionation of REE-rich

accessory minerals (monazite, xenotime. garnet, etc.; c.f. Liu et al., 2005; Irber, 1999) as no significant tetrad effect was observed in the unaltered.

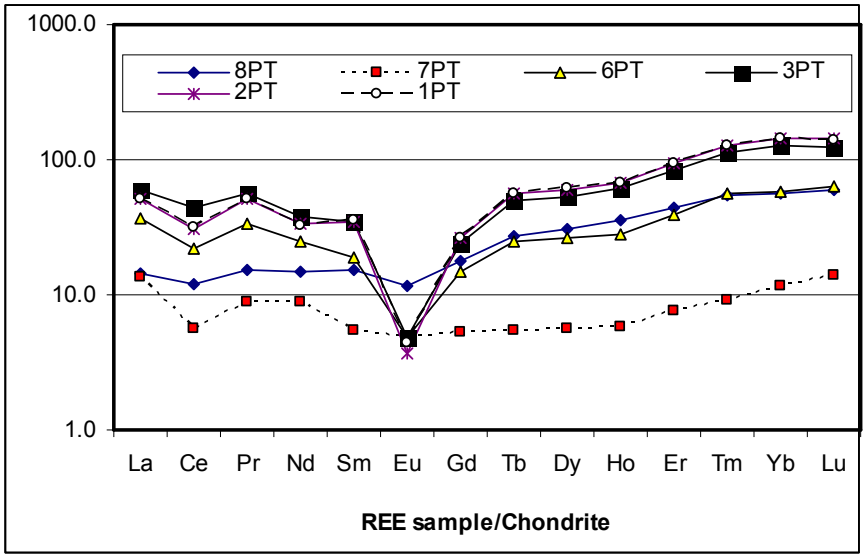

Fig. 12: Chondrite-normalized REE patterns of Abu Rusheid lamprophyre dyke.

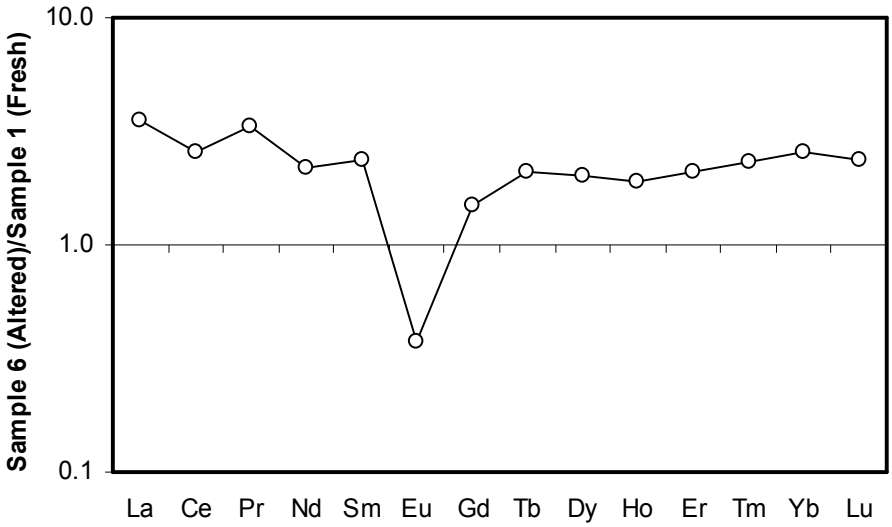

Fig. 13: Average 6 altered samples normalized to fresh sample.

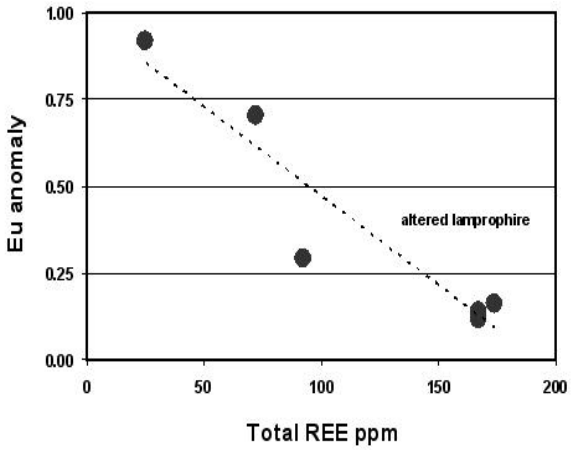

Fig. 14: Eu anomaly versus total REE in ppm.

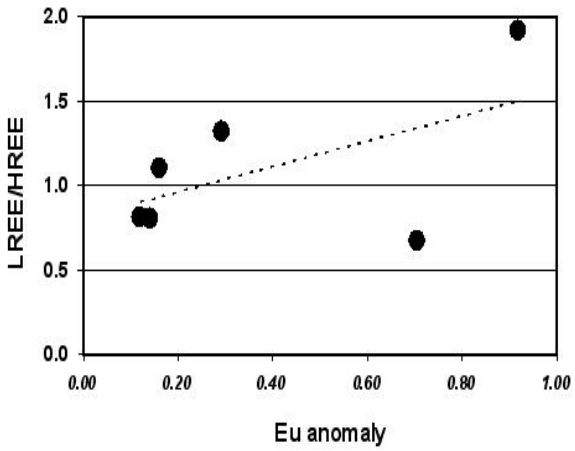

Fig. 15: Eu anomaly versus LREE/HREE ratio.

4- MINERALIZATION

Some minerals of the base metals (e.g., pyrite, chalcopyrite, sphalerite, covellite, arsenopyrite, zinc, willemite, zincite, franklinite, tungstenite and silver) in similar lamprophyre dyke in Abu Rusheid area but in close contact with the peraluminous granites were recorded by Ibrahim et al., (2007). Darwish (2008) recorded the occurrences of some secondary U – minerals in Abu Hawis shear zone.

Th -contents are higher than U- contents in all the analyzed samples. The U and Th contents of Abu Hawis range from (2.5-5.4 ppm) to (3.7- 6.9 ppm) whereas in Abu Rusheid range from (0.5-7.2 ppm) to (2.5-22.7 ppm), respectively. The accessory minerals responsible for the radioactivity are zircon, apatite, and allanite. The Th/U ratio in Abu Hawis (1.2-1.5) and Abu Rusheid (1-5.7) show a significant variation due to secondary mineralization of U.

5- DISCUSSIONS AND CONCLUSIONS

A- Abu Rusheid lamprophyre dyke

Abu Rusheid lamprophyre dyke has abnormally high contents of Zn (335 - >10000), Ni (206-517 ppm), Co (32-69 ppm) and Sn (55 -205 ppm). The ΣREE varies from 25 -174 ppm with negative Eu anomalies and LREE/HREE equal to 0.67-1.33. The REE pattern of lamprophyre displays the M-type tetrad effect (related to alteration). The presence of negative Ce anomaly in lamprophyre samples suggests precipitation from oxidized fluids.

The presence of box- works and clay minerals in E-W Abu Rusheid alkaline lamprophyre dyke is a good trap for mineralization and its source magma had ultra-potassic to rarely shoshonite nature**.** The lamprophyre was subjected to mineralized acidic and alkaline solution.

The high P-T lamprophyre dyke is characterized by high MgO (16 -18 wt%) and may be produced from a deep-seated tectono-metamorphic event incorporating melting of mantle with raised metamorphic grade due to emplacement of syn-tectonic rocks. The magma may be enriched by carbon dioxide which has an important role in fixation of mineralization.

Tourmaline crystals are formed from fluids generated by dehydration of pelitic and psammitic rocks during regional metamorphism (Henry and Guidotti, 1985) at temperatures of 500-700^{O} C (Mueller and Groves, 1997).

The presence of cordierite defines the beginning of the medium grade division of metamorphism at about 550^{O} C and up to 7k bar. In high-grade metamorphism, K-feldspar and sillimanite can be formed mainly by the break down of mica (Winkler, 1979).

The relation between the metamorphism and the emplacement of the syn-tectonic granitoids in the Abu Rusheid area raised the metamorphic grade of the country rocks to that of high-rank amphibolite facies and the metamorphic grade has remained frozen at such grade till the present day. The retrogressive minerals such as chlorite, sericite, zeolites and epidote are of very limited and local extent. The raising of thermal gradients in the country rocks caused the migmatization in many patches especially in places nearer to the granitoids and developed new metamorphic minerals (cordierite, sillimanite and kyanite) in lamprophyre dyke. Amphibole and phologopite are the most important reservoirs for LILE in the lithosphere (e.g. Foley et al., 1996; Ionov et al., 1997; Gre' goire et al., 2000)

B- Abu Hawis lamprophyre dyke

1- The Abu Hawis N-S lamprophyre dyke has 1-10m width and up to 1 km length with vertical dip, cutting peraluminous granite. Abu Hawis lamprophyre dike is barren from any mineralization. The dykes are grayish green to gray black and have lamprophyre

texture. The phynocrysts consist of hornblende, phologopite, and pyroxene, the groundmass consists essentially of a similar mineral assemblage. Calcite apatite, allanite and zircon are common accessories.

2- The lamprophyre dyke has an alkaline nature and its source magma is rich in LREE. It is depleted in Cr but enriched in U, Th, Rb and Zr relative to primitive mantle and its source magma, rich in LREE and LILE. The Nb/Ta ratio (16.6-18.3) and Zr/Hf ratio (39.7-43.5) are similar to primitive mantle (17.5 for Nb/Ta; 35-45 for Zr/Hf). The ∑REE varies from 292 to 370 ppm with weak Eu anomalies (Eu/Eu*= 0.85-1.09) and the LREE/HREE ratio ranging from 5.4 to 6.8. Abu Hawis lamprophyre does not show tetrad effect.

Acknowledgments

The authors would like to express their deep gratitude to ***Prof. Dr. Ahmed El Kammar,*** Prof. of Geochemistry, Cairo University for valuable discussion and comments.

REFERENCES

Alderton, D.H., Pearce, J.A. and Potts, P.J., 1980: Rare earth elements mobility during granite alteration: Evidence from Southwest England. Earth Planet. Sci. Lett. v. 49, p. 149-165.

Carlier, G., Lorand, J.P., Audebaud, E. and Kienast, J.R., 1997: Petrology of an unusual orthopyroxene-bearing minette suite from south-eastern Peru, Eastern Andean Cordillera: Al-rich lamproites contaminated by peraluminous granites. Journal of Volcanology and Geothermal Research, v. 75, p. 59-98.

Carmichael, I.S.E., Turner, F.J., Verhoogen, J., 1974: Igneous Petrology, McGraw-Hill. New York, 739 p.

Chung, S., Wang, K., Crawford, A., Kamenetsky, V.S., Chen, C., Lan, C. and Chen, C. 2001: High-Mg potassic rocks from Taiwan: implications for the genesis of orogenic potassic lavas. Lithos, v. 59, Issue 4, p. 153-170.

Cox, K.G., Bell, J.D. and Pankhurst, R.J., 1979: The interpretation of igneous rocks. George, Allen and Unwin, London.

Currie, K.L., Williams, P.R., 1993: An Archean calc-alkaline lamprophyre suite, northeastern Yilgarn Block, western Australia. Lithos, v. 31, p. 33–50.

Darwish, M., 2008: Uranium distribution in Abu Hawis shear zone, Central Eastern Desert, Egypt., Menofiya Univ. Bull.

Downes, H., Balaganskaya, E., Beard, A., Liferovich, R. and Demaiffe, D., 2005: Petrogenetic processes in the ultramafic, alkaline and carbonatitic magmatism in the Kola Alkaline Province: A review. Lithos, v. 85, p. 48-75.

Fitton, J.G., 1987: The Cameroon line, West Africa: a comparison between oceanic and continental alkaline volcanism. In: Fitton, J., G. and Upton, B. G. J. (Eds), Alkaline Igneous Rocks. Geol. Soc. Spec. Publ. v. 30, p. 273-291.

Foley, S.F., Jackson, S.E., Fryer, J.D., Greenough, G.A.J.,1996: Trace element partition coefficients for clinopyroxene and phlogophite in an alkaline lamprophyre from Newfoundland by LAM–ICP–MS. Geochim. Cosmochim. Acta, v. 60, p. 629–638.

Foley, S.F., Venturelli, G., Green, D.H., Toscani, L., 1987: The ultrapotassic rocks: characteristics, classification, and constraints for petrogenetic models. Earth-Sci. Rev. v. 24, p. 81-134.

Fowler, M.B., Henney, P.J., 1996: Mixed Caledonian appinite magmas: implications for lamprophyre fraction and high Ba-Srgranite genesis. Contributions to Mineralogy and Petrology, v.126, p. 199-215.

Ge, W.C. , Li, X.H. and Li, Z.X., 2001: Mantle Source and Tectonic Setting for the Volcanic Rocks from Danzhou Group in Longsheng Area, Northern Guangxi. Journal o f Chungchun University of Science and Technology, 31 (1) : 20 - 24 (in Chinese with English Abstract)

Gre'goire, M., Lorand, J.P., O'Reilly, S.Y., Cottin, J.Y., 2000: Armalcolite-bearing, Ti rich metasomatic assemblages in harzburgitic xenoliths from the Kerguelen Islands: implications from the oceanic mantle budget of high-filed strength elements. Geochim. Cosmochim. Acta, v. 64, p. 673–694.

Gaonach, H.H., Ludden, J.N and Picard,C.,1992: Highly alkaline lava in a proterozoic rift-zone: implications for Precambrian mantle metasomatic processes. Goel., v. 20, p. 24-250.

Hass, J.R., Shock, E.L. and Sassani, D.C., 1995: Rare earth elements in hydrothermal system: Estimates of standard partial model thermodynamic properties of aqueous complexes of the rare earth elements at high pressure and temperature. Geochim. Comochim Acta, v. 59, p. 4329-4335.

Henry, D.J. and Guidotti, C.V., 1985: Tourmaline as a petrogenetic indicator mineral: an example from the staurolite-grade metapelites of NW Maine. Am. Mineral., v. 70, p. 1-15.

Hoffmann, A.W. , Jochum, K.P. , Seufert, M., 1986: Nb and Pb in Oceanic Basalts: New Constraints on Mantle Evolution. Earth Planet. Sci. Lett. , v. 79, p. 33-45.

Huang, Z., Liu, C., Yang, H., Xu, C., Han, R., Xiao, Y., Zhang, B., Li, W., 2002: The geochemistry of lamprophyres in the Laowangzhai gold deposits, Yunnan Province, China: implications for its characteristics of source region. Geochemical Journal , v. 36, p. 91-112.

Ibrahim, M.E., El-Tokhi, M.M., Saleh G.M., and. Rashed, M.A., 2006: Lamprophyre bearing-REEs, South Eastern Desert, Egypt. 7th Intern. Conf. on Geochemistry, Fac. Sci., Alex. Univ., Alex., Egypt, 6-7 Sept..

Ibrahim, M.E., Abd El-Wahed, A.A., Rashed, M.A., Khaleal, F.M., Mansour, G.M. and Watanabe, K., 2007a: Comparative study between alkaline and calc-alkaline lamprophyres, Abu Rusheid area, south Eastern Desert, Egypt. The 10th Inter. Min., Petrol., and Metall. Eng. Conf., Assuit Univ., p. 99-115.

Ibrahim, M.E., Saleh, G.M., Hassan, M.A., El-Tokhi, M.M. and Rashed, M.A., 2007b: Geochemistry of lamprophyres bearing uranium mineralization, Abu Rusheid area, south Eastern Desert, Egypt. The 10th Inter. Min., Petrol., and Metall. Eng. Conf., Assuit Univ., p. 41-55.

Ibrahim M., Saleh G., Rashed M., and Watanabe, K., 2007c: Base metal mineralization in lamprophyre dykes at Abu Rusheid area, south Eastern Desert, Egypt. The 10th Inter. Min., Petrol., and Metall. Eng. Conf., Assuit Univ., p. 31-40. In: Wang, Hongzheng (Ed.), Accretion of the Asia. Seismological Publishing House, Beijing, p. 57–60.

Ionov, D.,A., Reilly, S.Y. and Griffin W.L., 1997: Volatile bearing minerals and lithophile trace elements in the upper mantle, Chem. Geol. V.141, p. 153-148.

Irber, W.,1999: The lanthanide tetrad effect and correlation with K/Rb, Eu/Eu.*Sr/Eu, Y/Ho, and Zr/Hf of evolving peraluminous granite suites, Geochimica et Cosmochimica Acta, v. 63, p. 489-508.

Le Maitre, R.W., 1989: A Classification of Igneous Rocks and Glossary of Terms: Recommendations of the International Union of Geological Sciences, Subcommission on the Systematic of Igneous Rocks. Blackwell, Oxford, 193 p.

Liu, C.Q., Zhan, H., 2005: The lanthanide tetrad effect in apatite from the Ataly No. 3 pegmatite, Xingjaing, China: an intrinsic feature of the pegmatitic magma. Chemical Geology, v. 214, p. 61-77.

Lu, F.X., Shu, X.X. and Zhao, C.H., 1991: A suggestion on Classification of lamprophyres Geo, Sci Chai Fengmei, Zhang Zhaochong , Mao Jingwen, Parat Abun du Kadir ,Wang Li Jin Dong Lianhui, Ya Husishou et al.

Madhavan, V., David, K., Mallikharjuna Rao, J., Chalapathi Rao, N.V. and Srinivas, M., 1998: Comparative study of lamprophyres from the Cuddapah Intrusive Province (CIP) of Andhra Pradesh, India. Journal of Geological Society of India, v. 52, p. 621-642.

Mahdy, A.I. and El Kammar, A.M., 2003: Geochemical partitioning of isovalents and tetrad effect of REE associating Episyenitization of Kab Amiri granites, Central Eastern Desert of Egypt. 5th Inter. Conference on the Geology of the Middle East, Cairo, Egypt, p. 111-125.

Masuda, A. Kawakami, O., Dohmoto, Y. and Takenaka, T., 1987: Lanthanide tetrad effect in nature: two mutually opposite types, W and M. Geochemical Journal, v. 21, p. 119-124.

McDonough, W.F. and Sun, S.S., 1988: A primitive mantle composition from xenoliths. Chem. Geol., v. 70, p. 12-27.

Mclennan, S.M., Fryer, B.J. and Yound, G.M., 1979: Rare earth elements in Huronian (lower Proterozoic) sedimentary rocks: Composition and evolution of the post-kenoran upper crust. Geoch. Cosmchim. Acta., v. 43, p. 375-388.

Moayyed, M., Moazzena, M., Calagari, A.A. Jahangiri, A. and Modjarrad, M., 2006: Geochemistry and petrogenesis of lamprophyric dykes and the associated rocks from Eslamy peninsula, NW Iran: Implications for deep-mantle metasomatism. Chemie der Erde, p. 1-14.

Moustafa, M.B., 2007: Geological and petrological investigations with special emphasis on uranium mineralization of Gabal Abu Hawis area, Central Eastern Desert, Egypt., M. Sc. Thesis, Fac. Sci., Menofiya Univ., Egypt, 141 p.

Mueller, A.G. and Groves, D.I., 1997: The classification of Western Australian greenstone-hosted gold deposits according to wallrock - alteration mineral assemblages. Ore Geol. Rev., v. 6, p. 291-331.

Prelevic, D., Foley, S.F., Cvetkovi, V. and Romer, R.L., 2004: Origin of Minette by Mixing of Lamproite and Dacite Magmas in Veliki Majdan, Serbia. Journal of Petrology, v. 45, p. 759-792.

Rock, N.M.S., 1991: Lamprophyres. Blackie, Glasgow, pp. 1–285. Rock, N.M.S., Groves, D.I., 1988. Can lamprophyres resolve the genetic controversy over mesothermal gold deposits. Geology, v. 16, p. 538-541.

Shu, X.X., 1994: The Research of Petrology of the Potassic Lamprophyres along the Western Border of Yangzi Platform. Acta Petrotogica Sinica , 10 (3) : 248 - 260 (in Chinese with English Abstract)

Streckeisen, A., 1979: Classification and nomenclature of volcanic rocks, lamprophyres, carbonatites, and melilitic rocks: recommendations and suggestions of the IUGS Sub commission on the Systematics of Igneous Rocks. Geology, v. 7, p. 331-335.

Sun, S.S. and Mc Donough, W.F., 1989: Chemical and isotopic systematics of oceanic basalts: implications for mantle compositions and processes. In: Saunders, A.D., Norry, M.J. (Eds.), Magmatism in the ocean basins. Geol. Soc. Long. Spec. Publ., v. 42, p. 313-345.

Tarney, J. and Weaver, B.L., 1987: Geochemistry and Petrogenesis of Early Proterozoic dyke swarms. In: Mafic dyke swarms (Edited by H.C. Halls and W.F. Fahrig), pp. 81-94, Geological association of Canda, Special paper 34.

Taylor, S.R., Arculus, R., Perfi, T. R. and Johnson, R.W., 1981: Island arc basalts .In R.B. Merrill and R. Ridings ,Eds., Basaltic Volcanism on the Terrestrial Planets, 193-213. Pergamon, New York.

Taylor, S.R. and McLennan, S.M., 1980: The rare earth elements evidence in Precambrian sedimentary rocks: Implication for crustal evolution in (ed. A. Kroner). Precambrian plate tectonic, Elsevier.

Thompson, R.N., 1986: Sources of basic magmas. Nature, v. 319, p. 448-449.

Thompson, R.N., Leat, P.T., Dickin, A.P., Morrison, M.A., Hendry, G.L. and Gibson, S.A., 1990: Strongly potassic mafic magmas from lithospheric mantle source during continental extension and heating: evidences from Miocene minettes of northwest Colorado, U.S.A. Earth and Planetary Science Letters, v. 98, p. 139–154.

Veklser, I.V., Dorfman, A.M., Kamenetsky, M. Dulski, P. and Dingwell, D., 2005: Partitioning of lanthandies and Y between immiscible silicate and fluoride melts, fluorite and cryolite and the origin of the lanthanide tetrad effect in igneous systems. Geohimica et Cosmochimica Acta, v. 69, p. 2847-2860.

Whalen, J.B., Jenner, G.A., Longstaff, F.J., Robert, F. and Galiépy, C., 1996: Geochemical and isotopic (O, Nd, Pb and Sr) constraints on A-type granite petrogenesis based on the Topsails igneous suite, Newfoundland Appalachians. J. Petrology, v. 37, p. 1463-1489.

Winkler, H.G.F., 1979: Petrogenesis of metamorphic rocks. Springer Verlag, New York, London, 348 p.

Zhang, Y., Chen, B., Shao, J.A., and Zhai, M.G., 2003: Geochemistry and origin of late Mesozoic lamprophyre dykes in Aihang mountains, north China. Acta Petrologica ET Mineralogica, v. 22, p. 29-33 (in Chinese with English abstract).

Zhao, Z., Xiong, X., Han, X., Wang, Y., Wang, Q., Bao, Z., and Jahn, B., 2002: Controls on the REE tetrad effect in granites: Evidence from the Qianlishan and Baerzhe Granites, China. Goeochemical Journal, v. 36, p. 527-543.